Parasitology

cambridge.org/par

Glucose-restriction increases *Trichomonas vaginalis* cellular damage towards HeLa cells and proteolytic activity of cysteine proteinases (CPs), such as TvCP2

Jesús F. T. Miranda-Ozuna*, Luis Alberto Rivera-Rivas*, Rosa Elena Cárdenas-Guerra, Mar Sarai Hernández-García, Sarahí Rodríguez-Cruz, Arturo González-Robles, Bibiana Chavez-Munguía and Rossana Arroyo

Departamento de Infectómica y Patogénesis Molecular, Centro de Investigación y de Estudios Avanzados del Instituto Politécnico Nacional (CINVESTAV-IPN), Av. IPN # 2508, Col. San Pedro Zacatenco, Delg. Gustavo A. Madero, CP 07360, Mexico City, Mexico

Research Article

*These authors contributed equally to this work.

Cite this article: Miranda-Ozuna JF T, Rivera-Rivas LA, Cárdenas-Guerra RE, Hernández-García MS, Rodríguez-Cruz S, González-Robles A, Chavez-Munguía B, Arroyo R (2019). Glucose-restriction increases *Trichomonas vaginalis* cellular damage towards HeLa cells and proteolytic activity of cysteine proteinases (CPs), such as TvCP2. *Parasitology* **146**, 1156–1166. https://doi.org/10.1017/S0031182019000209

Received: 15 August 2018
Revised: 5 February 2019
Accepted: 7 February 2019
First published online: 12 March 2019

Key words:
Apoptosis induction; cellular damage; cysteine proteinases; cytotoxicity; glucose regulation; *Trichomonas vaginalis*

Author for correspondence:
Rossana Arroyo, E-mail: rarroyo@cinvestav.mx

Abstract

Trichomonas vaginalis induces cellular damage to the host cells (cytotoxicity) through the proteolytic activity of multiple proteinases of the cysteine type (CPs). Some CPs are modulated by environmental factors such as iron, zinc, polyamines, etc. Thus, the goal of this study was to assess the effect of glucose on *T. vaginalis* cytotoxicity, proteolytic activity and the particular role of TvCP2 (TVAG_057000) during cellular damage. Cytotoxicity assays showed that glucose-restriction (GR) promotes the highest HeLa cell monolayers destruction (~95%) by trichomonads compared to those grown under high glucose (~44%) condition. Zymography and Western blot using different primary antibodies showed that GR increased the proteolytic activity, amount and secretion of certain CPs, including TvCP2. We further characterized the effect of glucose on TvCP2. TvCP2 increases in GR, localized in vesicles close to the plasma membrane and on the surface of *T. vaginalis*. Furthermore, pretreatment of GR-trichomonads with an anti-TvCP2r polyclonal antibody specifically reduced the levels of cytotoxicity and apoptosis induction to HeLa cells in a concentration-dependent manner. In conclusion, our data show that GR, as a nutritional stress condition, promotes trichomonal cytotoxicity to the host cells, increases trichomonad proteolytic activity and amount of CPs, such as TvCP2 involved in cellular damage.

Introduction

Trichomonas vaginalis is the causative agent of human trichomoniasis, the most common non-viral sexually transmitted infection worldwide, affecting ~276.4 million people annually (Poole and McClelland, 2013). This flagellated protist is responsible for severe health complication, such as chronical inflammation (vaginitis, urethritis and prostatitis), infertility, increasing the risk of prostate and cervical cancer, and facilitating the infection and transmission of the human immunodeficiency virus (HIV) (Petrin *et al.*, 1998).

The cellular and molecular mechanisms of *T. vaginalis* pathogenesis have not been clearly elucidated due to the multifactorial nature of its virulence mechanisms described up to date. Particularly, multiple molecules have been identified in the cellular damage caused by *T. vaginalis,* such as porins (Fiori *et al.*, 1993), phospholipases (Lubick and Burgess, 2004) and proteinases localized on the parasite surface or secreted into the extracellular medium, depending on the environmental conditions (Figueroa-Angulo *et al.*, 2012). *Trichomonas vaginalis* has multiple proteinases, mainly of the cysteine type (CPs), differentially modulated by iron, playing crucial roles in the virulence of *T. vaginalis*, in cytoadherence (TvLEGU-1) (Arroyo and Alderete, 1989; Rendón-Gandarilla *et al.*, 2013), cytotoxicity (TvCP39 and TvCP65) (Alvarez-Sánchez *et al.*, 2000; Ramón-Luing *et al.*, 2011), haemolysis (TvCP4) (Cárdenas-Guerra *et al.*, 2013), apoptosis induction (TvCP2, TvCP3, TvCP4 and TvCPT) (Sommer *et al.*, 2005), among others. Additionally, trichomonad CPs are found in the vaginal secretions of patients with trichomoniasis, some of which are immunogenic (Hernández *et al.*, 2014; Arroyo *et al.*, 2015). During vaginal infection, trichomonads are constantly exposed to stress conditions throughout the menstrual cycle, competition for nutrients with the vaginal microflora, and host immune response, among others. However, *T. vaginalis* adapts and responds to environmental changes, differentially modulating the expression of multiple genes, including those encoding virulence factors, to maintain a chronic infection (Figueroa-Angulo *et al.*, 2012). Glucose is the primary carbon source for *T. vaginalis* under both anaerobic and aerobic conditions. Thus, the energy generation through glycolysis is vital to the maintenance of a trichomonal chronic infection. The major source of glucose in the vaginal fluid is from the glycogen derived from vaginal epithelial cells through the action of α-glucosidase and β-amylase (Stafkova *et al.*, 2018). We recently reported that *T. vaginalis* is exposed to different glucose levels (0.3–36.65 mM) during vaginal infection of women with trichomoniasis. We also reported that

CAMBRIDGE UNIVERSITY PRESS

glucose promotes trichomonad growth and increases the adherence levels of parasites to laminin and fibronectin (Miranda-Ozuna *et al.*, 2016). *Trichomonas vaginalis* also activates survival mechanism, such as metabolic reprogramming, enhancing antioxidant ability and autophagy, as a response to nutritional stress by glucose restriction (Huang *et al.*, 2014, 2017). These data suggest that glucose is also an essential nutrient for *T. vaginalis*; however, its effects on trichomonal pathogenesis have not been explored yet.

Here, we assessed the effect of nutritional stress by glucose-restriction (GR) on the trichomonal cytotoxicity and apoptosis induction of HeLa cells and proteolytic activity involved in cellular damage. GR condition increases the cytotoxicity levels of *T. vaginalis* and the proteolytic activity released by *T. vaginalis* during host–parasite interaction with HeLa cell monolayers. Furthermore, TvCP2 plays a key role in cytotoxicity and apoptosis induction to HeLa cells under GR conditions.

Materials and methods

Parasites and HeLa cell cultures

Trichomonas vaginalis parasites from the fresh clinical isolate CNCD188 (Alvarez-Sánchez *et al.*, 2000) were cultured for 1 week by daily passages in trypticase-yeast extract (TY) medium supplemented with 25 mM glucose (MERCK) [standard glucose concentration in the regular medium TYG; normal glucose (NG)] and 10% heat-inactivated bovine serum (HIBS) after incubating at 37 °C for 20 h. For growing parasites in different glucose concentrations, TY-HIBS medium was either supplemented with 50 mM glucose (high glucose; HG) or not supplemented with extra glucose (GR), containing ⩽1 mM glucose derived from medium components (Miranda-Ozuna *et al.*, 2016). HeLa cells were grown in Dulbecco's Modified Eagle Medium (DMEM) (Gibco Laboratories, Grand Island, NY, USA) supplemented with 10% HIBS for 48 h at 37 °C in a 5% CO_2 atmosphere to obtain confluent HeLa cell monolayers (Alvarez-Sánchez *et al.*, 2007).

Preparation of protein extracts and gel electrophoresis separation by sodium dodecyl sulfate-polyacrylamide gel electrophoresis (SDS-PAGE)

Total protein extracts (TPE) were obtained from parasites (2×10^7) grown under both glucose (HG and GR) conditions by 10% trichloroacetic acid (TCA) precipitation at 4 °C overnight (ON) and analysed by SDS-PAGE on 12% polyacrylamide gels. Similarly, protease-resistant extracts (PRE) were obtained from parasites (2×10^7) grown under both glucose conditions without protease inhibitors, which leaves the proteolytic activity intact for detection. Briefly, parasites suspended in PBS pH 8 were lysed with 0.5% sodium deoxycholate (DOC) for 20 min at 4 °C, centrifuged at 16 000 × ***g*** for 30 min at 4 °C, and analysed by SDS-PAGE on 12% polyacrylamide gels. The proteolytic activity from PRE or DMEM-TYG medium (20 μL) obtained after 60 min parasite–HeLa cell interaction was analysed by substrate SDS-PAGE on 12% polyacrylamide gels co-polymerized with 0.2% gelatin (Bio-Rad Laboratories, Hercules, CA, USA). Proteinases were renatured with 2.5% Triton X-100 and activated with 100 mM sodium acetate buffer, pH 4.5, containing 0.1% β-mercaptoethanol for 12 h or 18 h at 37 °C, respectively, as described by Cárdenas-Guerra *et al.* (2013). Gels were Coomassie brilliant blue (CBB) stained to show the proteolytic activity as white bands against a blue background.

Western blot (WB) assays

For WB assays, TPE or PRE from parasites (2×10^7) grown under HG or GR conditions were separated by SDS-PAGE, blotted onto nitrocellulose (NC) membranes (0.2 µm pore size; Bio-Rad), blocked with 10% nonfat dried milk in PBS-Tween 20 [PBS pH 7 with 0.1% Tween 20 (PBS-T20)], and incubated with different primary antibodies (all diluted in PBS-T20): anti-TvCP2r (1:2000 dilution), anti-TvCP3r (1:2000 dilution), anti-TvCP4r (1:1000 dilution), anti-TvCP12r (1:2000 dilution), anti-TvCP39r (1:1000 dilution), anti-TvLEGU-1r (1:500 dilution), anti-Tv-CatDr (1:200 dilution) and anti-TC-2r (1:200 dilution) for 18 h at 4 °C. After incubation for 1 h at 37 °C with a peroxidase-conjugated goat anti-rabbit secondary antibody (1:3000 dilution in PBS-T20 with 5% nonfat dried milk; Bio-Rad), the reactive bands were developed using a chemiluminescence system (SuperSignal West Pico Chemiluminescent Substrate; Thermo Scientific-Pierce). Images were captured with a ChemiDoc XRS System (Bio-Rad) and analysed using the Quantity One software (Bio-Rad). Alpha-enolase protein (TvENO) detected with an anti-TvENOr antibody (1:2000 dilution in PBS-T20) was used as a loading or secretion control, since it is not affected by glucose. Triosephosphate isomerase (TvTIM), detected with an anti-TvTIMr antibody (1:1000 dilution in PBS-T20) was used as a control protein upregulated by glucose (Miranda-Ozuna *et al.*, 2016). These experiments were performed at least two independent times with similar results.

Cytotoxicity assay

Cytotoxicity assays were performed by a colorimetric method as described by Alvarez-Sánchez *et al.* (2000) with some modifications. Briefly, parasites grown under HG or GR conditions were suspended in DMEM:TY interaction medium [2:1 (vol/vol)] without HIBS, supplemented with 50 mM glucose (HG) or without glucose (GR), according to the parasite glucose growth condition. Parasites (2×10^5 well^{-1}) were added to confluent HeLa cell monolayers on 96-well microtiter plates (~4×10^4 cells well^{-1}) at a 5:1 ratio (parasite: HeLa cell) and incubated for 15, 30 and 60 min at 37 °C in a 5% CO_2 atmosphere, washed 5× with PBS at RT, and HeLa cell monolayer destruction was assessed using light microscopy and spectrophotometric quantification at 570 nm. The interaction medium after 60 min host–parasite interaction was recovered, centrifuged and the supernatant was analysed by zymography for the presence of trichomonad secreted proteinases. Control parasites in the interaction medium without serum and with or without glucose (TYG:DMEM or TY:DMEM) were monitored for cell viability at the same incubation time of the assay by the trypan blue exclusion method. Parasite viability was maintained between 99 and 98% throughout the assay (up to 60 min) under both interaction media.

For cytotoxicity inhibition experiments, parasites grown under GR conditions were pre-incubated with increasing concentrations (0, 25, 50, 100 and 200 μg mL^{-1}) of an anti-TvCP2r immunoglobulin G (IgGs) (purified by the caprylic acid method, as previously reported; Sánchez-Rodríguez *et al.*, 2018) for 30 min at 37 °C, before interaction with confluent HeLa cell monolayers on 96-well microtiter plates for 30 min at 37 °C in a 5% CO_2 atmosphere. The same concentrations of preimmune (PI) rabbit serum IgGs were used as a negative control. Untreated parasites were taken as 100% cytotoxicity. The experiment was performed in triplicate at least three independent times, with similar results.

Apoptosis assays

Apoptosis assays (Annexin V-FITC and DNA fragmentation assay) were performed using the same protocol described above for cytotoxicity inhibition experiments. After incubation of *T. vaginalis* with confluent HeLa cell monolayers on 96-well microtiter plates for 30 min at 37 °C in a 5% CO_2 atmosphere and washed 5 times with PBS at room temperature (RT), remnant

https://doi.org/10.1017/S0031182019000209 Published online by Cambridge University Press

HeLa cell monolayers were labeled for 15 min using the Annexin V-fluorescein isothiocyanate (FITC) Fluorescence Microscopy Kit (BD Pharmingen), following the manufacturer's recommendations. The FITC fluorescent signal from apoptotic HeLa cells was analysed by epifluorescence microscopy (Nikon, Japan) (Sommer *et al.*, 2005) and quantitated by a spectrofluorometric analysis (SpectraMax Gemini EM spectrofluorometer).

For DNA fragmentation assay, after incubation of *T. vaginalis* with confluent HeLa cell monolayers on 6-well microtiter plates (at a 4:1 ratio) for 30 min at 37 °C in a 5% CO_2 atmosphere, the supernatant was recovered and centrifuged. The cells attached in the plate and in the pellet were lysed with the lysis buffer (10 mM Tris-HCl pH 7.4, 5 mM EDTA, 0.2% Triton X-100). DNA was pretreated with RNase A (50 μg mL^{-1}) and proteinase K (1 mg mL^{-1}), recovered by phenol-chloroform extraction and precipitated with ethanol and 3 M sodium acetate. Normal-grown parasites and HeLa cells treated with 5% H_2O_2 for 30 and 60 min at 37 °C in a 5% CO_2 atmosphere were used as positive controls. The DNA was analysed by electrophoresis in 2% agarose gels (Abcam Protocols, 2018).

In vitro secretion assays

The *in vitro* secretion assays were performed as described by Cárdenas-Guerra *et al.* (2013) with few modifications. Parasites grown under HG or GR condition were harvested, washed three times with PBS pH 7 and suspended (1×10^6 parasites mL^{-1}) in PBS supplemented with 50 mM glucose or without glucose, according to the parasite growth condition (HG or GR, respectively). The parasites were incubated at 37 °C for 60 min, parasite viability was measured by the trypan blue exclusion method, and the supernatant containing secretion products (SP) was clarified by centrifugation at 900 × ***g*** and filtered through a 0.22 µm NC membrane. The proteins were precipitated with 10% TCA at 4 °C ON, separated by SDS-PAGE on 12% polyacrylamide gels, blotted onto NC membrane, and analysed by WB assay to confirm the presence of TvCP2 in the SP. To identify TvCP2 by mass spectrometry (MS) in the *in vitro* SP, the protein band of interest was manually excised from the CBB-stained gel and a matrix-assisted laser desorption/ionization (MALDI)-time of flight (TOF) MALDI-TOF/TOF MS analysis was performed at the Protein Core Facility, (CINVESTAV-IPN, Unidad Irapuato).

Immunolocalization of TvCP2 by indirect immunofluorescence assays (IFA)

To determine the localization of TvCP2 under different glucose conditions, IFA and confocal microscopy analyses were performed using parasites grown under HG and GR conditions and an anti-TvCP2r antibody. For TvCP2 localization, parasites were fixed with 4% formaldehyde in PBS for 20 min at RT on coverslips, washed two times with 20 mM NH_4Cl in PBS (NH_4Cl-PBS), two times with 0.2% bovine serum albumin (BSA) in PBS (PBS-BSA) and two times with PBS before permeabilization with 0.02% Triton X-100 in PBS for 5 min at RT. Parasites were then incubated with an anti-TvCP2r antibody or PI serum (both at a 1:100 dilution) for 1 h at RT, washed five times with PBS, and incubated with a FITC-conjugated anti-rabbit secondary antibody (1:100 dilution) (Thermo Scientific-Pierce) for 1 h at RT. For nuclei staining, the coverslips were mounted with Vectashield- 4′,6-diamidino-2-phenylindole (DAPI) mounting solution (Vector Laboratories, Burlingame, CA) and the parasites were analysed by confocal microscopy using a Zeiss microscope and ZEN 2012 software (Carl Zeiss, Germany). For lysosome staining, live parasites (1×10^6 parasites mL^{-1}) grown under both glucose conditions (HG and GR) were incubated with 2 μM Lysotracker Red DND-99 (Invitrogen) following the manufacturer's instructions for 30 min at 37 °C with gentle shaking. Parasites were then washed, fixed and processed as described for IFA with the anti-TvCP2r antibody.

Immunogold labelling and transmission electron microscopy (TEM)

Parasites grown under HG and GR conditions were fixed with 4% formaldehyde-0.2% glutaraldehyde in serum-free DMEM, dehydrated in ethanol, embedded in LR White resin (London Resin Co. Ltd., Berkshire, UK) and polymerized under UV light at 4 °C for 18 h. Ultrathin sections were mounted on mesh nickel grids, incubated with an anti-TvCP2r primary antibody (1:30 dilution), for 18 h, washed, incubated with a 15 nm gold particle-conjugated goat anti-rabbit IgGs secondary antibody (Ted Pella, Inc., Reeding, CA, USA) for 1 h at RT, and contrasted with uranyl acetate and lead citrate. As a negative control, the secondary antibody alone was used. Ultrathin sections were analysed by TEM in a JEM-1011 transmission electron microscope (JEOL Ltd., Tokyo, Japan).

Scanning electron microscopy (SEM)

After parasite–HeLa cell interaction in TY:DMEM interaction medium without serum for 45 min at 37 °C, samples were fixed in 2.5% glutaraldehyde in cacodylate buffer for 30 min at 37 °C, washed with PBS and milli-Q water, dehydrated in ethanol, critical point-dried with CO_2 in a Sandri-780 dryer (Tousimis®) and coated with gold using a JFC-1100 ionizer (JEOL Ltd., Tokyo, Japan). The samples were analysed with a JEOL-JSM 7100 F scanning electron microscope (JEOL Ltd., Tokyo, Japan).

Statistical analysis

Statistically significant differences between means were determined by analysis of variance (ANOVA) using GraphPad Prism 5.0. The data were analysed by one-way ANOVA using the Tukey method comparing all pairs of columns ($P < 0.05$) for Figs 1, 2 and 5. The scores showing statistical significance are indicated in the figures with an asterisk. The corresponding *P* values are indicated in the figure legends.

Results

Effect of glucose on the cytotoxicity levels and the amount and proteolytic activity of T. vaginalis *proteinases*

To assess the effect of glucose on the cytotoxicity of *T. vaginalis,* parasites grown under both (GR and HG) glucose conditions were incubated with confluent HeLa cell monolayers and the levels of cellular destruction were determined by a colorimetric method. Interestingly, the optical microscopy (Fig. 1A) and spectrophotometric analyses (Fig. 1B) showed that parasites under GR conditions exhibited the highest levels of monolayers destruction (~95%) compared to parasites under HG conditions (~44%) after 60 min interaction. These differences were significant.

In addition to contact-dependent cytotoxicity, *T. vaginalis* secretes molecules with a proteolytic activity that could contribute to cellular damage. To confirm this, we performed zymograms of the PRE and supernatants obtained after 60 min of HeLa–Tv interaction under both (GR and HG) glucose conditions (Fig. 1C). Our results showed the presence of four main bands (~90-, ~66-, ~34- and ~25-kDa) with proteolytic activity released after host–parasite interaction under both glucose conditions (Fig. 1C, lanes 3 and 4). However, under GR condition the proteolytic activity bands were more intense, especially the ~66 kDa

https://doi.org/10.1017/S0031182019000209 Published online by Cambridge University Press

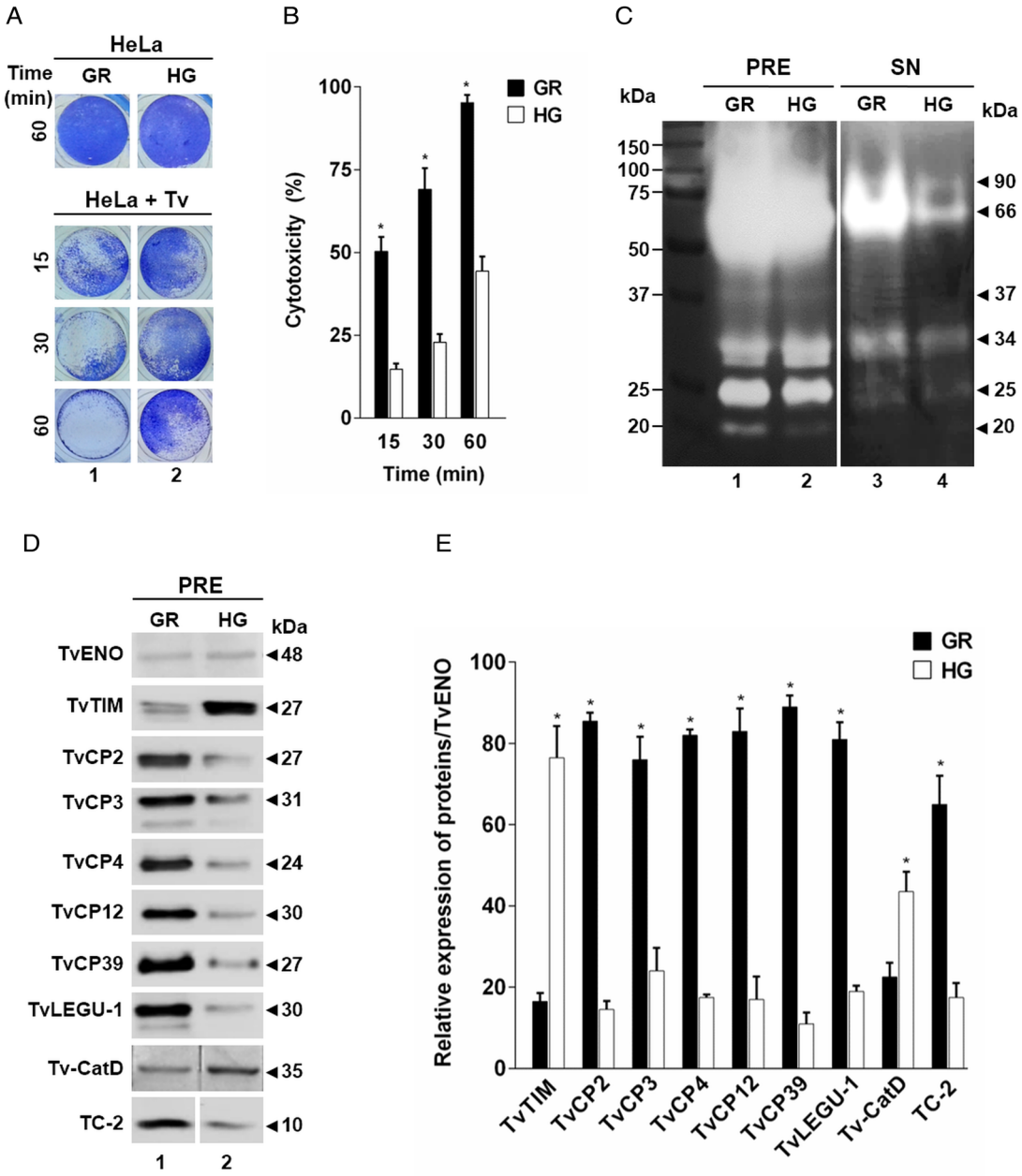

Fig. 1. Effect of glucose on the cytotoxicity levels, proteolytic activity and amount of different proteins of *Trichomonas vaginalis*. (A) Cytotoxicity assays to show HeLa cell monolayers integrity by staining with crystal violet dye, after 15, 30 and 60 min interaction with *T. vaginalis* under glucose-restricted (GR) (Lane 1) or high glucose (HG) (lane 2) conditions. HeLa cell monolayers incubated 60 min under both GR and HG conditions, but without *T. vaginalis* were used as 100% monolayer integrity controls. (B) Percentage of cytotoxicity levels on HeLa cells induced by *T. vaginalis* at different times (15, 30 and 60 min), under GR (black bars) or HG (white bars) conditions determined by spectrophotometric analysis of the eluted dye from HeLa cell monolayers. (C) Zymogram of proteinase-resistant extracts (PRE) (lanes 1 and 2) or supernatants (SN) (lanes 3 and 4) obtained after interaction of HeLa cell monolayers with parasites grown under GR (lanes 1 and 3) or HG (lanes 2 and 4) conditions for 60 min at 37 °C and 5% CO_2 atmosphere. (D) WB assays of proteinase-resistant extracts (PRE, 35 μg per lane) from parasites grown under GR (lane 1) or HG (lane 2), transferred onto NC membrane and incubated with different primary antibodies against recombinant proteinases of *T. vaginalis* (TvCP2, TvCP3, TvCP4, TvCP12, TvCP39, TvLEGU-1 and Tv-CatD). An anti-trichocystatin 2 (TC-2r) antibody recognizes a 10-kDa band of an endogenous inhibitor of CPs, TC-2. An anti-enolase (TvENOr) antibody that recognizes a 48-kDa band was used as a control protein (TvENO) not affected by glucose. An anti-triosephosphate isomerase (TvTIMr) antibody that recognizes a 27-kDa band was used as a control protein (TvTIM) for a positive glucose modulation. (E) Densitometric analysis of the bands detected by WB (D) using the Quantity One software (Bio-Rad). The bar graphs show the relative amounts of TvTIM, TvCP2, TvCP3, TvCP4, TvCP12, TvCP39, TvLEGU-1, Tv-CatD and TC-2 proteins normalized to the level of the TvENO protein. For B and E, the error bars indicate the standard deviation (SD) of three and two independent experiments, respectively. The asterisk (*) shows significant differences ($P < 0.05$) as determined by ANOVA. Arrowheads show the proteolytic activity bands in the zymogram (C) and the molecular weight of protein bands detected by WB in kDa (D).

band, than under HG condition. Zymograms from PRE (Fig. 1C, lanes 1 and 2) under both glucose conditions (GR and HG) were used as controls of the effect of glucose on the total trichomonad proteolytic activity. These results showed that certain CPs are released by *T. vaginalis* during HeLa–Tv interaction mainly under GR conditions.

To determine the effect of glucose on the amount of proteins related to trichomonal virulence, particularly with cellular damage, PRE from parasites grown under both (GR and HG) glucose conditions were analysed by WB assays using different anti-proteinases antibodies (Fig. 1D). Our results showed an increase in the amount of proteinases TvCP2, TvCP3, TvCP4, TvCP12, TvCP39, TvLEGU-1 and the endogenous inhibitor of CPs, trichocystatin-2 (TC-2), under GR condition (Fig. 1D, lane 1) compared to the reduced amount of Tv-CatD and TvTIM under the same GR condition, because these are two glucose

https://doi.org/10.1017/S0031182019000209 Published online by Cambridge University Press

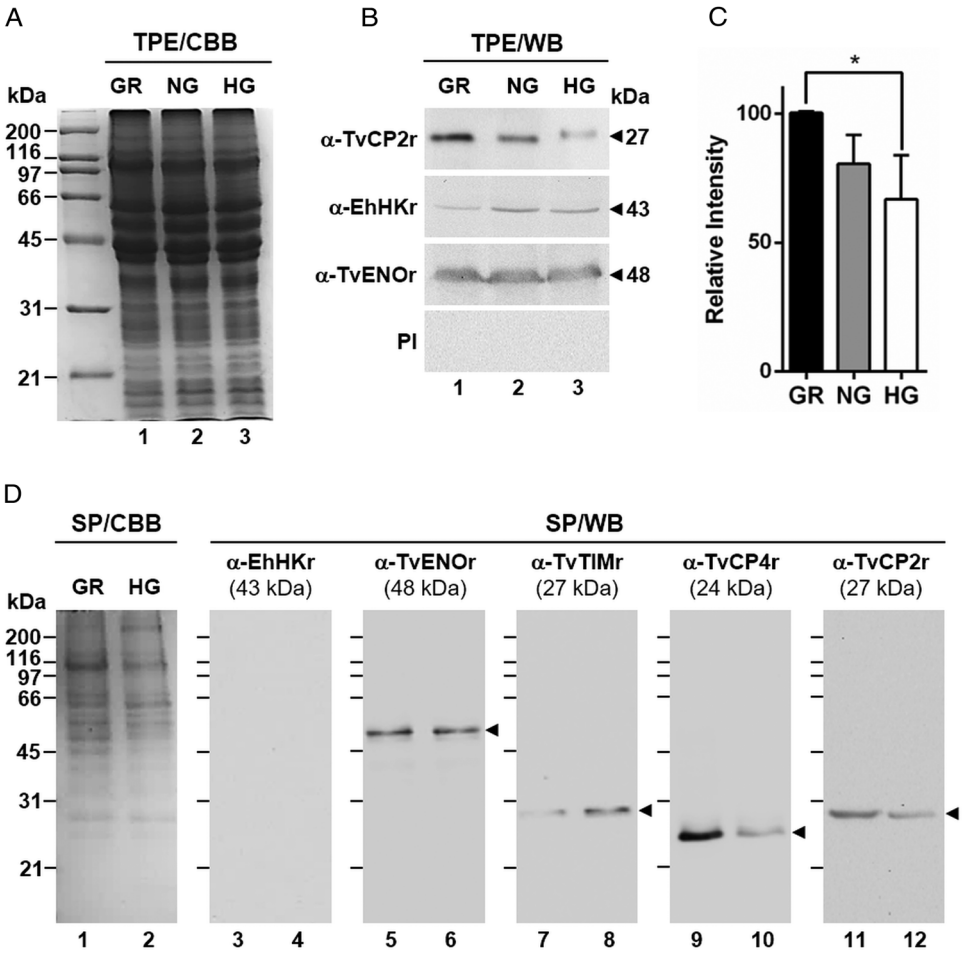

Fig. 2. Glucose-restricted (GR) condition up-regulates the amount and *in vitro* secretion of TvCP2 by *Trichomonas vaginalis*. (A) SDS-PAGE and Coomassie brilliant blue (CBB) staining of 12% polyacrylamide gels were performed to assess the total protein extracts (TPE) from parasites grown under GR (lane 1), NG (lane 2) and HG (lane 3) conditions. (B) For WB assays, duplicated gels from the panel (A) transferred onto NC membranes were incubated with different primary antibodies, including an anti-TvCP2r antibody (*α*-TvCP2r; 1:2000 dilution) that recognized a 27-kDa band corresponding to the native TvCP2 protein. An anti-hexokinase antibody (*α*-EhHKr; 1:1000 dilution) that recognized a 43-kDa band was used as a control protein (TvHK) for glucose-induced modulation. An anti-enolase (*α*-TvENOr) antibody that recognized a 48-kDa band was used as a control protein (TvENO) not affected by glucose. A preimmune rabbit serum (PI) (1:1000 dilution) was used as a negative control. (C) Densitometric analysis of the bands detected by WB (B) using the Quantity One software (Bio-Rad). The bar graphs show the relative amount of TvCP2 protein, under the three glucose conditions (GR, NG and HG), normalized to the level of the TvENO protein, which was used as a loading control. The error bars indicate standard deviations (SDs) of three independent experiments. The asterisk (*) show significant differences ($P < 0.05$), as determined by ANOVA. (D) SDS-PAGE and CBB staining of 12% polyacrylamide gels of proteins present in secretion products (SP) of *T. vaginalis,* obtained in GR (lane 1) and HG (lane 2), concentrated with 10% TCA precipitation and transferred onto NC membranes for WB assays. The *α*-EhHKr antibody (1:1000 dilution) was used as a control of a protein (TvHK) that is not secreted under both glucose conditions (GR and HG) (lanes 3 and 4). The *α*-TvENOr antibody was used as a control of a secreted protein (TvENO) that is not affected by glucose condition (lanes 5 and 6). The *α*-TvTIMr antibody was used as a control of a secreted protein (TvTIM) induced by glucose (lanes 7 and 8). The *α*-TvCP4r antibody was used as a control of a secreted protein (TvCP4) downregulated by glucose (lanes 9 and 10). The *α*-TvCP2r antibody was used to follow the secretion of TvCP2. Arrowheads show the expected protein bands detected by WB.

upregulated proteins, used as positive controls of the HG effect (Fig. 1D, lane 2). These differences corroborated by densitometric analysis (Fig. 1E) of the bands detected by WB normalized against the TvENO band, used as a loading control, were significant ($P < 0.05$) for all the proteins studied.

GR induces expression and secretion of TvCP2 in T. vaginalis.

The cysteine proteinase TvCP2 was previously identified as part of a 30 kDa band (CP30) with proteolytic activity found in *in vitro* SP of *T. vaginalis* composed of four CPs (CP2, CP3, CP4 and CPT), negatively regulated by iron and involved in cytotoxicity and apoptosis induction to vaginal epithelial cells (Sommer *et al.*, 2005; Kummer *et al.*, 2008). In addition, we recently reported that TvCP2 is one of the trichocystatin-3 (TC-3; an endogenous CP inhibitor) targeted CPs (Sánchez-Rodríguez *et al.*, 2018). Together, these data suggest that TvCP2 could be involved in cytotoxicity. However, TvCP2 has not been characterized yet as an individual CP. Thus, we followed TvCP2 in further experiments to investigate the effect of glucose in this particular CP and its possible role in cytotoxicity.

By WB using PRE from parasites grown under GR and HG conditions and an anti-TvCP2r antibody, we found that the amount of TvCP2 is reduced by glucose (Fig. 1D). To confirm the glucose negative effect, TPE from parasite grown under GR (⩽1 mM), NG (25 mM) and HG (50 mM) conditions were analysed by SDS-PAGE (Fig. 2A) and WB assays using an anti-TvCP2r antibody (Fig. 2B). Our results show the highest amount of the 27-kDa TvCP2 band in parasite proteins from GR condition (Fig. 2B, lane 1) compared with those from NG and HG conditions (Fig. 2B, lanes 2 and 3). These differences corroborated by densitometric analysis of the WB TvCP2 bands normalized against the TvENO band (Fig. 2C) were significant ($P < 0.05$). WB with an anti-EhHKr antibody, using the same TPE extracts, was performed as a control of a protein positively regulated by glucose, showing an opposite effect to TvCP2 (Fig. 2B). PI rabbit serum was used as a negative control for WB (Fig. 2B). Thus, these data show that the amount of TvCP2 is reduced by glucose.

https://doi.org/10.1017/S0031182019000209 Published online by Cambridge University Press

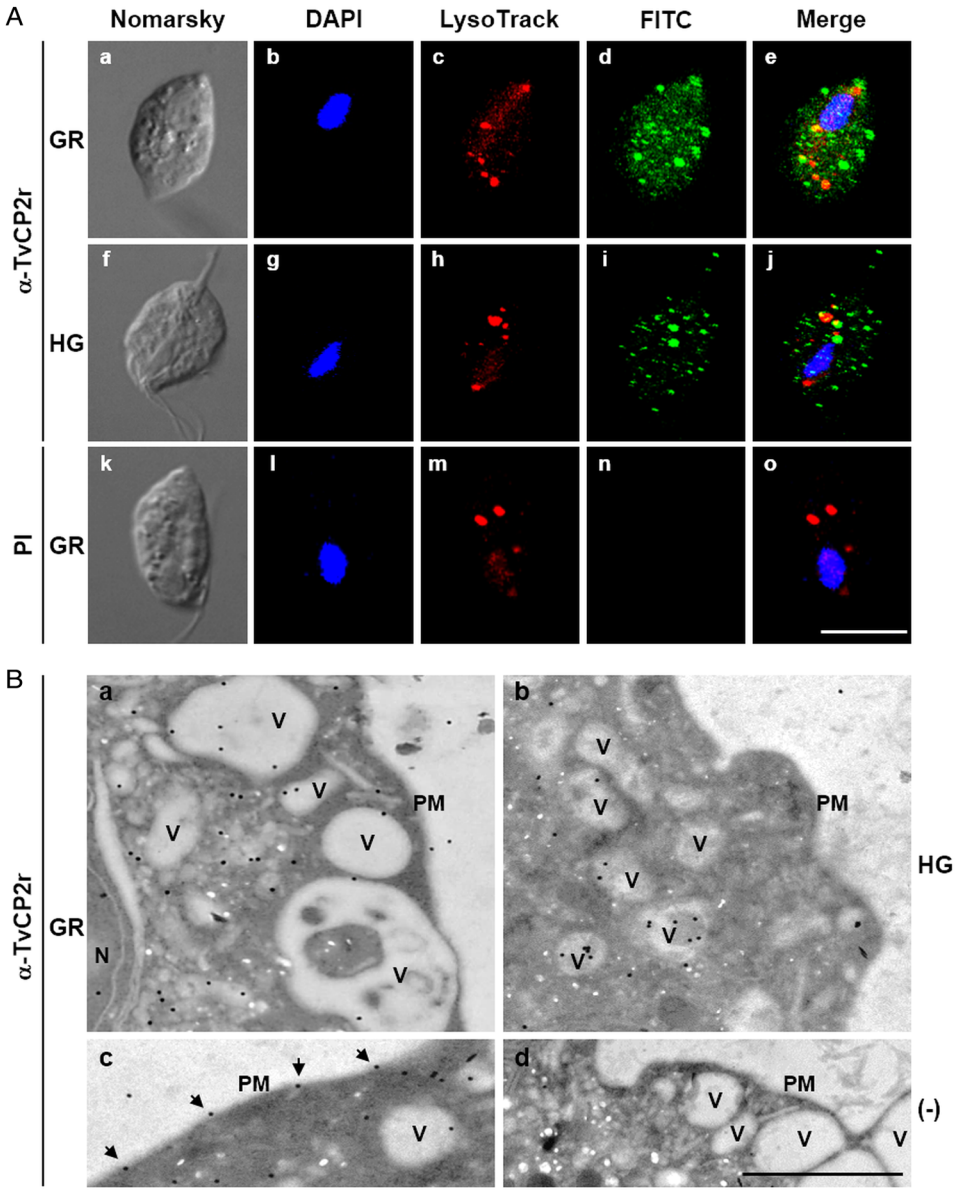

Fig. 3. The TvCP2 proteinase is localized in cytoplasmic vesicles and on the surface of *Trichomonas vaginalis*. (A) Nomarsky microscopy and indirect immunofluorescence to detect the cytoplasmic, lysosomal and vesicle localization of TvCP2 in permeabilized parasites grown under GR (a–e) and HG (f–j) conditions. Before fixation, live parasites were incubated for 30 min at 37 °C with LysoTracker red to stain lysosomes. Parasites were then fixed, blocked and incubated with a primary anti-TvCP2r antibody (1:100 dilution) followed by a FITC-conjugated secondary antibody (1:100 dilution). As a negative control, permeabilized parasites grown under GR condition incubated with preimmune (PI) rabbit serum (1:100 dilution) followed by a FITC-conjugated secondary antibody (k–o) were used. The confocal microscopy (Zeiss) images show nuclei labelled with DAPI (in blue), lysosomes (acid vesicles) stained with LysoTracker (in red) and TvCP2 labelled with FITC (in green). The merged images show the low levels of co-localization between TvCP2 and parasite lysosomes (in yellow). Bar size: 10 µm. These experiments were performed two independent times, with similar results. (B) Possible vesicle trafficking routes to the plasma membrane of TvCP2. TEM analysis of immunogold labelling of ultrathin sections of parasites grown under GR (panels a, c and d) and HG (panel b) conditions using a primary α-TvCP2r antibody at 1:30 dilution and a secondary antibody conjugated to 15 nm gold particles. The TEM images show parasites in GR conditions directly incubated with a secondary antibody conjugated to gold particles as a negative control (panel d). In general, TvCP2 gold labelling free in the cytoplasm, in cytoplasmic vesicles (V), vesicles close to the plasma membrane (PM) and on the parasite surface (arrows). N, nucleus. Bar: 1 µm.

To determine whether glucose affects the secretion of TvCP2, we performed an *in vitro* secretion and WB assays (60 min at 37 °C) using parasites grown under GR and HG glucose conditions and an anti-TvCP2r antibody. Parasites showed 95–97% viability at the end of the secretion assay. Figure 2D shows that TvCP2 is secreted under both glucose conditions (Fig. 2D, lanes 11 and 12). The TvCP2 band was more intense in the SP of parasites in the GR (Fig. 2D, lane 11) than in the HG conditions; whereas the control TvENO band showed similar intensity in both glucose condition, suggesting that secretion of TvENO is not affected by glucose levels (Fig. 2D, lanes 5 and 6). In contrast, the TvTIM band showed greater intensity in the HG (Fig. 2D, lanes 8) than in the GR conditions; whereas the TvCP4 band showed greater intensity in the GR (Fig. 2D, lane 9) than in the HG conditions. Both proteins were used as positive controls of secreted proteins under both glucose conditions. As a negative control of secretion, the TvHK was not detected by the specific antibody, as expected (Fig. 2D, lanes 3 and 4). The CBB-stained control gel showed the protein profile of SP of parasites in the GR and HG conditions (Fig. 2D, lanes 1 and 2). The presence of TvCP2 in the *in vitro* secretion products detected by the anti-TvCP2r antibody (Fig. 2D) was confirmed by MS analysis. Five peptides with identical masses to TvCP2 (TVAG_057000) were identified by MALDI-TOF/TOF MS analysis that represents 22% TvCP2 sequence coverage (Supplementary Fig. S1). Thus, these data show that TvCP2 is part of the released products of live trichomonads promoted by glucose restriction condition.

TvCP2 is localized in the cytoplasm, vesicles and on the surface of T. vaginalis

To assess the cellular localization of TvCP2 in trichomonads grown under different glucose conditions, we performed IFA on formaldehyde-fixed and permeabilized parasites using an anti-TvCP2r antibody. By confocal microscopy, higher fluorescence signal (in green) on cytoplasm (free and in vesicles) and close to the surface of parasites grown under GR (Fig. 3A, panels a–e) than under HG conditions (Fig. 3A, panels f–j) was observed, which was further confirmed by immunogold localization TEM images (Fig. 3B). As a negative control, in parasites incubated with PI serum (Fig. 3A, panels k–o) no green fluorescent was observed, as expected.

To explore whether TvCP2 may have a typical lysosomal localization, similar to other cathepsin-L CPs, we performed co-localization assays using the anti-TvCP2r antibody and LysoTracker-red DND-99 as a lysosomal marker. Figure 3A shows (in the merged

https://doi.org/10.1017/S0031182019000209 Published online by Cambridge University Press

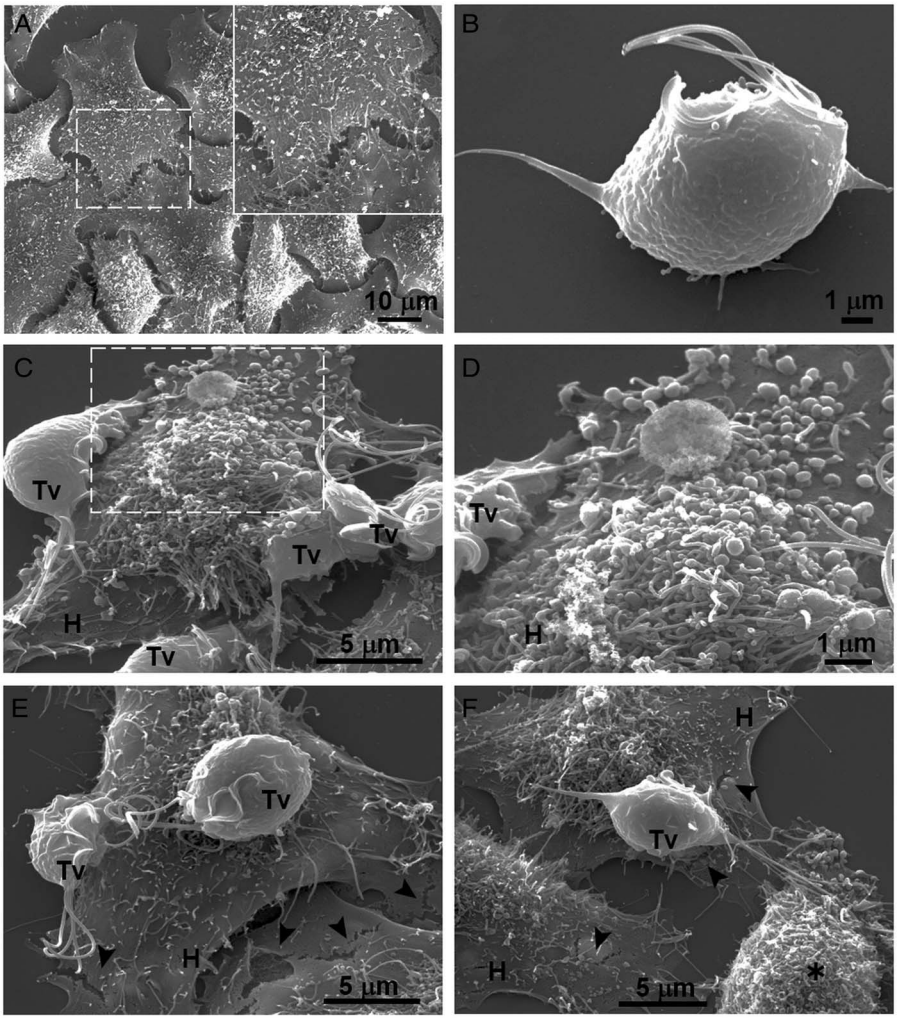

Fig. 4. SEM observation of a HeLa cells monolayer interaction with *Trichomonas vaginalis* grown in GR condition. (A) Control HeLa cells monolayer with a zoom of their surface (white frame). (B) Control *T. vaginalis* (Tv), keeps an ovoid shape with free flagella. (C) Interaction of HeLa cells (H) monolayer and *T. vaginalis*, the blebbing cells and stress fibres are observed during the interaction. (D) Higher magnification of the blebbing cell during the interaction (framed area in C). (E) Disruption on the HeLa cell surface during the interaction (black arrowhead). (F) A parasite over a HeLa cell (H) while flagella interact with another HeLa cell that is rounded (asterisk), disruption on HeLa cell surface (arrowheads).

images) very low levels of TvCP2/lysosomal co-localization in parasites under both glucose conditions (Fig. 3A, panels e and j; in yellow) with a Pearson's correlation coefficient of 0.43 for GR and 0.27 for HG conditions. These data suggest that TvCP2 is not a lysosomal CP. Thus, the TvCP2-positive vesicles (in green) could correspond to secretory vesicles (Fig. 3A), mainly under GR conditions.

TEM and immunogold localization assays of parasites grown under both glucose conditions confirmed the subcellular localization of TvCP2. Parasites under GR condition showed localization in the cytoplasm (62%), inside vesicles with different sizes (30%), or on the plasma membrane (6%) (Fig. 3B, panels a and c). Similarly, in trichomonads under HG condition, TvCP2 showed cytoplasmic localization (33%), inside vesicles (54%), or on the plasma membrane (4%) (Fig. 3B, panel b). Interestingly, in parasites under GR condition, TvCP2 was also localized in electron-lucent vesicles close to the plasma membrane (Fig. 3B, panel a) that could correspond to putative secretory vesicles. Moreover, the detection of the gold label on the parasite membrane confirms the surface localization of TvCP2 mainly under GR condition (Fig. 3B, panel c, black arrowheads). The secondary antibody used as a negative control did not show any gold labelling, as expected (Fig. 3B, panel d).

TvCP2 plays a key role in the trichomonal cytotoxicity through apoptosis induction in HeLa cells.

Our results showed that GR increases the cytotoxicity levels of *T. vaginalis* to HeLa cell monolayers (Fig. 1). In addition, GR increases the amount and promotes surface localization and secretion of TvCP2 (Figs 2 and 3), suggesting a possible role of TvCP2 in the trichomonal cytotoxicity modulated by glucose starvation. To explore this hypothesis, we assessed the protective effect of an anti-TvCP2r antibody against trichomonal cytotoxicity. We first check by SEM the type of cellular damage inflicted by *T. vaginalis* grown under GR conditions to HeLa cell monolayers during the parasite:host interaction (Fig. 4). Figure 4A shows the morphology of control HeLa cells monolayer and the integrity of the HeLa cells surface with microvilli (zoomed image). The morphology of a control parasite grown in the GR condition is also shown (Fig. 4B). Figure 4C–F show the HeLa cells drastic morphological changes due to the interaction with *T. vaginalis*. Parasites firmly adhered to cells conserved the ovoid shape (Tv), whereas the cells in contact with parasites presented blebs and long stress fibres, both markers of cell stress and apoptosis induction (Fig. 4C and D). Besides, HeLa cells with or without direct contact with parasites also presented rupture of the cell membrane (Fig. 4E and F, black arrowhead). Rounded HeLa cells in contact with parasite flagella were also observed as another type of damage inflicted by trichomonads (Fig. 4F, asterisk). These results show that the interaction between HeLa cells and GR-parasites induced severe cellular damage that could be related to apoptosis induction.

Thus, to evaluate the participation of TvCP2 in this type of cellular damage, live parasites grown under GR condition were preincubated with increased concentrations of the anti-TvCP2r IgGs (0–200 μg mL^{-1}) before interaction with HeLa cell monolayers expecting some degree of protection. Figure 5A shows up to ~60% reduction in trichomonal cytotoxicity using 100 and

https://doi.org/10.1017/S0031182019000209 Published online by Cambridge University Press

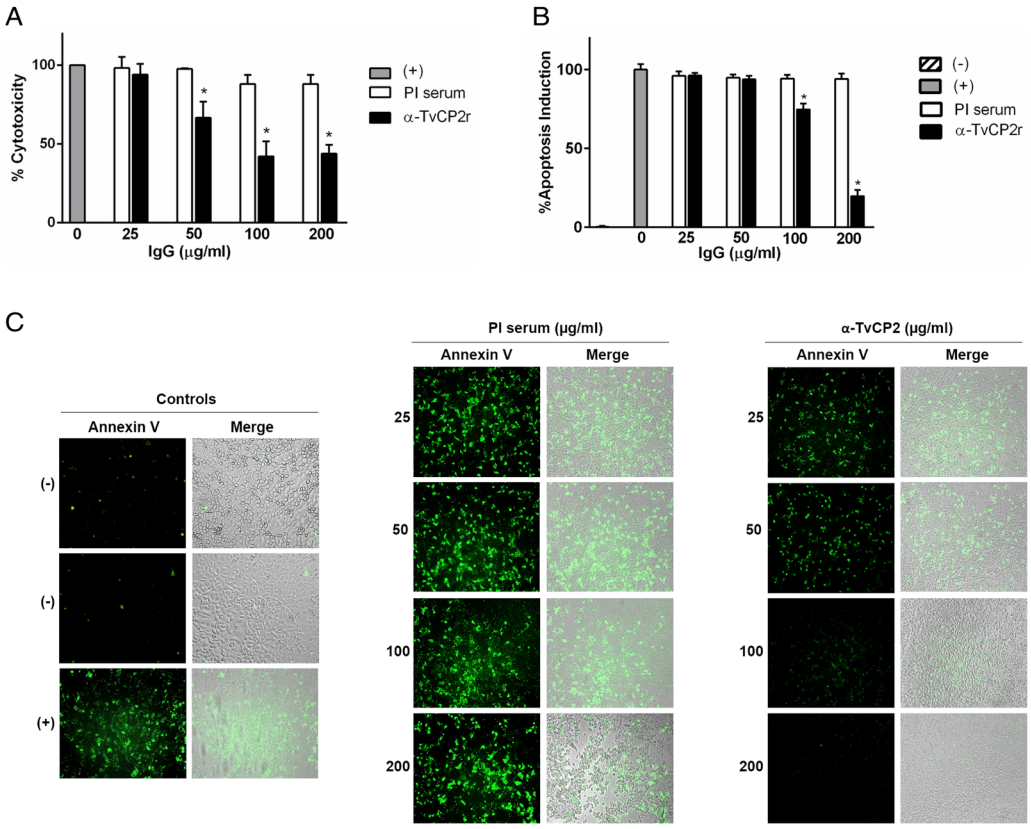

Fig. 5. TvCP2 participates in the cellular damage towards HeLa cells due to apoptosis induction. (A) Cytotoxicity inhibition assay performed with 2×10^5 live parasites grown under GR condition and preincubated with increasing concentrations (0–200 μg mL^{-1}) of anti-TvCP2r or PI serum purified IgGs followed by incubation with HeLa cell monolayers (4×10^4 cells well^{-1}) at 5:1 ratio. HeLa cell monolayers without parasites were used as a negative control. HeLa cell monolayers with parasites grown under GR without antibody treatment were used as a positive control (+) and considered as 100% cytotoxicity levels. (B) Apoptosis inhibition assay was performed similarly to the cytotoxicity inhibition assay. After incubation with live parasites, cell monolayers were incubated with FITC-conjugated Annexin V. Annexin V fluorescence signal (in green) was quantified using a SpectraMax Gemini EM spectrofluorometer. Each point in the bar is the mean of the percentage of cell monolayer destruction or apoptosis induction of representative experiments with triplicate samples. The error bars indicate standard deviations (SDs) of three independent experiments. The Annexin V fluorescence signal of HeLa cell monolayers without parasites but incubated in the interaction media (DMEM:TY) (mock) were used as a negative control (–). HeLa cell monolayers incubated with parasites grown under GR without antibody treatment were used as a positive control (+) and considered as 100% apoptosis induction. The asterisk (*) shows significant differences ($P < 0.05$), as determined by ANOVA. (C) Annexin-V fluorescence signal was also observed by epifluorescence microscopy (Nikon). In addition to the other assay controls described in (B), HeLa cell monolayers before the host–parasite interaction were used as an extra negative control (–). The green label indicates apoptotic cells accompanied by cellular damage.

200 μg mL^{-1} anti-TvCP2r IgGs compared with the same concentrations of PI serum IgGs used as a negative control, which showed great monolayer destruction (Fig. 5A).

We further hypothesized that cellular damage that leads to cell death of HeLa cell monolayers by live trichomonads is due to apoptosis induction, and TvCP2 is one of the molecules participating in this process. To test this hypothesis, we performed an apoptosis inhibition assay by the Annexin V-FITC method in the presence of increasing concentrations of purified anti-TvCP2r or PI serum IgGs. Figure 5B and C show the apoptosis induction to HeLa cell monolayers by parasites grown under GR condition as a strong Annexin V green label and wide destruction of HeLa cell monolayers, which was taken as 100% apoptosis induction. The damage of HeLa cell monolayer and Annexin V label was reduced in a concentration-dependent manner up to ~80% by the anti-TvCP2r IgGs, but not by the PI serum IgGs used as a negative control (Fig. 5B and C). These differences were significant (Fig. 5B).

We further analysed the HeLa cells damage caused by *T. vaginalis* through the DNA degradation assays by agarose gel electrophoresis. Figure 6A shows high molecular size bands indicative of the integrity of HeLa cells and trichomonads genomic DNA before the host–parasite interaction used as controls. As a positive control of DNA degradation for both type of cells, we induced apoptosis by treatment with 5% H_2O_2 for 30 and 60 min at 37 °C (Singh *et al.*, 2007) and observed the fragmentation/degradation of both genomic DNAs. As expected, in HeLa cells after H_2O_2 treatment a DNA laddering with multiple bands was observed; whereas in trichomonads, the H_2O_2 treatment induced DNA degradation observed as a smear (Fig. 6A, lanes 5–6). Analysis of the genomic DNA after the parasite–host cell interaction showed a massive degradation and the absence of the high molecular size DNA band (Fig. 6B, lane 3) compared with the control DNA bands (Fig. 6B, lanes 1–2). However, a certain degree of protection of the genomic DNA band was observed after the interaction of anti-TvCP2r IgG-pretreated parasites with HeLa cell monolayers (Fig. 6B, lane 4) compared with the interactions with PI serum IgGs-pretreated parasites (Fig. 6B, lane 5) used as a control.

These data confirmed the participation of TvCP2 in the trichomonal cytotoxicity due to apoptosis induction to HeLa cell monolayers, as previously suggested (Sommer *et al.*, 2005; Kummer *et al.*, 2008).

Discussion

Glucose is the primary carbon and energy source for *T. vaginalis*. We recently reported that *T. vaginalis* is exposed to different glucose levels (0.3–36.65 mM) during vaginal infection of women with trichomoniasis (Miranda-Ozuna *et al.*, 2016). Compared to the lowest value of glucose detected in vaginal secretion

https://doi.org/10.1017/S0031182019000209 Published online by Cambridge University Press

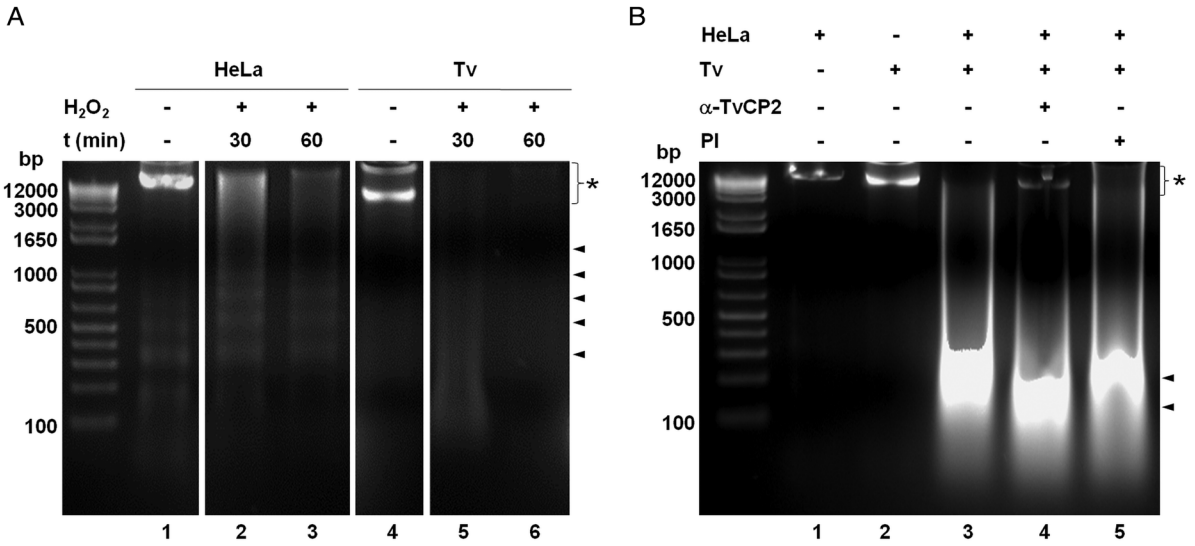

Fig. 6. *Trichomonas vaginalis* induces DNA damage to HeLa cells. (A) DNA degradation assay performed to assess the DNA damage due to *T. vaginalis* interaction. (A) Lane 1, HeLa cells genomic DNA. Lanes 2 and 3, positive controls of HeLa cell DNA damage induced by 5% H_2O_2 treatment for 30 and 60 min, respectively. Lane 4, *T. vaginalis* genomic DNA. Lanes 5 and 6, positive control of trichomonad DNA damage induced by 5% H_2O_2 treatment for 30 and 60 min, respectively. Arrowheads point to the DNA bands. Asterisk shows the large size genomic DNA band. (B) Inhibition of DNA degradation assay performed with live parasites (4×10^{6}) grown under GR condition and pre-incubated with 200 μg mL^{-1} of anti-TvCP2r or PI serum purified IgGs followed by incubation with HeLa cell monolayers (1×10^{6} cells $well^{-1}$) for 30 min (lanes 4 and 5). Genomic DNA from HeLa cell monolayers without parasites and from parasites grown under GR condition were used as controls of intact DNA (lanes 1 and 2, respectively). Genomic DNA obtained from the interaction of HeLa cell monolayers with parasites grown under GR without antibody treatment was used as a positive control of DNA degradation (lane 3). DNA was analysed by electrophoresis in 2% agarose gels. Asterisk shows the presence of large size genomic DNA.

(0.3 mM) of patients with trichomoniasis, ⩽1 mM glucose, used in *in vitro* assays as the GR condition, it is representative of the lowest glucose concentration detected during trichomonal infection.

In vitro studies showed that under metabolic stress by GR, *T. vaginalis* activates several adaptive mechanisms, such as metabolic reprogramming, enhancing antioxidant ability and autophagy as a cell survival strategy (Huang *et al.*, 2014, 2017). In this work, we focused on studying the effect of GR on the *T. vaginalis* cytotoxicity, as another cell survival strategy for the acquisition of glucose and nutrients from the host cell.

Here, we report that glucose negatively regulates trichomonal cytotoxicity. Particularly, we observe almost total destruction of HeLa cell monolayers by *T. vaginalis* under GR conditions, in a contact-dependent manner, suggesting that *T. vaginalis* activates its cytotoxicity mechanism in response to nutritional stress by glucose. A similar cytotoxic effect induced by GR conditions has been reported in other parasites as *Entamoeba histolytica,* supporting that glucose has an important role in parasites virulence modulation (Tovy *et al.*, 2011).

In addition to cell contact, the cytotoxicity of *T. vaginalis* also involves secreted molecules to the extracellular medium, such as porins, phospholipases and proteinases that contribute to cellular damage (Fiori *et al.*, 1993; Lubick and Burgess, 2004). Thus, in this work, we explored the effect of glucose on the activity of proteinases released during the interaction of *T. vaginalis* with HeLa cell monolayers. Zymograms show the presence of at least 4 bands with proteolytic activity in both glucose conditions (GR and HG) released during host–parasite interaction and cellular destruction. Interestingly, the highest proteolytic activity was observed in a 66-kDa band under GR conditions, suggesting that certain proteolytic activity could be linked with the high cytotoxicity levels of *T. vaginalis* under GR conditions. The CP-dependent cytotoxicity has been related to a 65-kDa (TvCP65) (Alvarez-Sánchez *et al.*, 2000) and a 39-kDa (TvCP39) (Hernández-Gutiérrez *et al.*, 2003, 2004; Ramón-Luing *et al.*, 2011) proteolytic activities modulated by environmental factors such as iron, zinc, polyamines and other unknown factors that participate in *T. vaginalis* virulence (Figueroa-Angulo *et al.*, 2012), such as glucose as described in here.

Trichomonas vaginalis exhibits high levels of proteolytic activity, mediated mainly by CPs (Hernandez *et al.*, 2014; Arroyo *et al.*, 2015). Some CPs are differentially modulated by iron and play diverse biological roles in trichomonal pathogenesis. In this study, we found that glucose negatively regulates the expression of six CPs: TvCP2, TvCP3, TvCP4, TvCP12, TvCP39 and TvLEGU-1 at the protein level. Interestingly, some of these CPs have been localized on the cell surface of or secreted by *T. vaginalis,* participating in different steps of the host cellular damage, such as cytoadherence (TvLEGU-1) (Rendón-Gandarilla *et al.*, 2013), haemolysis (TvCP4) (Cárdenas-Guerra *et al.*, 2013), cytotoxicity (TvCP12 and TvCP39) (Hernández-Gutiérrez *et al.*, 2003, 2004) and apoptosis (the secreted CP30 complex: CP2, CP3, CP4 and CPT) (Kummer *et al.*, 2008; Sommer *et al.*, 2005). Our results suggest that some of the CPs negatively modulated by glucose could be responsible for the high cytotoxicity levels of *T. vaginalis* under GR conditions.

We also found that glucose also reduced the amount of one of the endogenous cystatin-like CP inhibitors, TC-2, previously identified in the active degradome of *T. vaginalis* to be associated with TvCP39 (Ramón-Luing *et al.*, 2011; Puente-Rivera *et al.*, 2014). Their principal function is cellular protection from an exacerbated proteolytic activity, suggesting that overexpression of TC-2 under GR condition could be related with the increase in the CPs amount, proteolytic activity and cytotoxic effect of *T. vaginalis* toward host cells. In addition to its association with TvCP39, it is possible that the TC-2 inhibitor binds to other CPs as a regulatory mechanism of the endogenous trichomonad CP proteolytic activity under GR conditions.

An opposite effect to the CPs expression was observed for the trichomonad aspartic proteinase Tv-CatD. We found that glucose positively regulates the expression of Tv-CatD at the protein level. The Tv-CatD was recently reported as a proteinase that degrades human haemoglobin (Mancilla-Olea *et al.*, 2018). *In vivo*, the erythrocytes are an important source of glucose and haemoglobin for

https://doi.org/10.1017/S0031182019000209 Published online by Cambridge University Press

T. vaginalis. We hypothesize that glucose and haemoglobin levels are increased during menstrual flux, positively affecting the expression of Tv-CatD that could be involved in haemolysis.

In vitro studies show that *T. vaginalis* causes cell detachment followed by cellular destruction as a result of apoptosis induced by secreted CPs of the 30 kDa region (CP2, CP3, CP4 and CPT). Here, we reported that the amount of TvCP2, TvCP3 and TvCP4 increased under GR, a stress condition that promotes the destruction and death of the host cells in up to 30–60 min interaction. Thus, we selected to follow TvCP2 as one of the molecules responsive to glucose, to confirm the cytotoxicity and apoptosis induction under GR condition. First, we used TPE from parasites grown under different glucose condition (GR, NG and HG) to confirm that the amount of TvCP2 and its secretion increased by GR conditions. The negative effect of glucose in cellular damage described in here is similar to the negative influence of iron in cytotoxicity and apoptosis induction (Sommer *et al*., 2005; Kummer *et al*., 2008).

The highest proteolytic activity of *T. vaginalis* is in acid lysosomes. Therefore, it is expected that cathepsin L-like CPs are localized in this cellular compartment. We investigate the effect of glucose on the lysosomal localization of TvCP2. Our results show that TvCP2 does not have lysosomes as the main localization in trichomonads as other cathepsin-L CPs do. TvCP2 main localization was in different size vesicles close to the plasma membrane, suggesting that TvCP2 was in secretory vesicles. The vesicles localization of TvCP2 was confirmed by TEM microscopy that shows the highest gold particle labelled in parasites grown under GR compared to those under HG conditions. The localization of TvCP2 in secretory vesicles is supported by the *in vitro* secretion results and consistent with the presence of TvCP2 as part of the CP30 *in vitro* secreted proteolytic activity (Sommer *et al*., 2005).

The parasite–HeLa cell interaction analysed by SEM showed that the apoptosis induction in HeLa cell by parasites in the GR condition is due to the detachment and rounding of HeLa cells and the presence of blebbing cells, a characteristic during the execution phase of apoptosis (Mills *et al*., 1999, Charras, 2007). Moreover, we observed the presence of stress fibres and rupture of the cell membrane due to the mechanical stress and cytotoxic effect induced in a short period (30 min) compared with the effect induced by fresh Tv isolates (Midlej and Benchimol, 2010).

The results of cytotoxicity and apoptosis inhibition, using the anti-TvCP2r antibody, confirm that TvCP2 is used by trichomonads to induce cellular destruction, damage to DNA and cell death of the HeLa cell monolayers under GR condition. Our results show a 60 and 80% of cytotoxicity and apoptosis inhibition, respectively, and certain protection of the HeLa cells genomic DNA degradation by the anti-TvCP2r antibody, showing the participation of other trichomonad molecules that contribute to cellular damage, a multifactorial virulence mechanism. Further studies will be necessary to identify and characterize the mechanism of apoptosis induction by TvCP2.

Analysing the events that occur in the apoptosis cascade, we can note that the apoptosis process has 4 stages: (1) Induction, (2) Early stage, (3) Mid-stage, (4) Late stage. The induction stage is divided into 2 pathways such as the intrinsic pathway, mediated by mitochondria in response to internal stimuli such as DNA or plasma membrane damage and the extrinsic pathway, mediated by extracellular death receptors, for example, FasL to CD95 (Elmore, 2007). Our results suggest the activation of the apoptosis pathway during the trichomonads–HeLa cells interaction because we observed HeLa cell plasma membrane asymmetry (Annexin-V fluorescence signal) and DNA damage, and some inhibition of these processes when the parasites were preincubated with the anti-TvCP2r IgGs before the interaction with HeLa cells.

However, we could not analyse the deeper apoptosis pathway such as caspase-3 activation because our assay conditions do not allow analysis of longer interaction times as previously reported (Sommer *et al*., 2005; Kummer *et al*., 2008) due to the high cytotoxicity levels and proteolytic activity of the fresh trichomonad isolate used in this study, properties that were greatly enhanced by glucose restriction studied in here (Miranda-Ozuna *et.al*., 2016). These particular conditions drove the HeLa cells to rapid cell detachment, lost of the monolayer, cell rounding and blebbing and massive cellular destruction in less than 1 h that appears to be not enough time to detect caspase-3 activation as previously shown for SiHa cells after 4 h (Quan *et at*., 2017). More experiments will be needed to elucidate the apoptosis process during the interaction between trichomonads and HeLa cells mediated by glucose. Nevertheless, the participation of other trichomonad molecules during the apoptosis cannot be discarded.

Same as glucose, iron also plays an important role in trichomonal cytotoxicity and apoptosis induction (Alvarez-Sánchez *et al*., 2007; Kummer *et al*., 2008). The parasite responds to iron fluctuations by changing the gene expression of CPs. For example, *tvcp4* and *tvcp12* mRNAs are upregulated and downregulated by iron, respectively, by a posttranscriptional regulatory mechanism mediated by RNA–protein interactions described for both mRNAs (Solano-Gonzalez *et al*., 2007; Torres-Romero and Arroyo, 2009; Arroyo *et al*., 2015; Figueroa-Angulo *et al*., 2015). Based on that, we could hypothesize that a similar mechanism mediated by RNA–protein interactions could also participate in the glucose-related gene expression regulation of trichomonad CPs. However, an unknown mechanism cannot be discarded.

It is also clear from recent data (Huang *et al*., 2014; Miranda-Ozuna *et al*., 2016; Mancilla-Olea *et al*., 2018; Stafkova *et al*., 2018) that glucose gene expression regulation is just starting to be unveiled as an attractive new field of research in *T. vaginalis*. No doubt that the new findings will shed some light in understanding the complex biology that *T. vaginalis* uses for survival during infection in the highly changing vaginal environment throughout the menstrual cycle.

In summary, our findings demonstrated that GR is another nutritional stress condition that promotes trichomonal cytotoxicity to the host cells, by increasing the amount and proteolytic activity of CPs such as TvCP2, which plays an important role in the apoptosis induction during cellular damage.

Supplementary materials. The supplementary material for this article can be found at https://doi.org/10.1017/S0031182019000209.

Author ORCIDs. Rossana Arroyo, 0000-0002-8193-9700.

Acknowledgments. We would like to thank Carlos Vázquez-Calzada for his help with the confocal microscopy analysis at the Confocal microscopy facility of the DIPM-CINVESTAV-IPN. We also thank QFB Leticia Avila-González for her technical assistance in maintaining parasite cultures, Lizbeth I. Salazar-Villatoro and Anel Lagunes-Guillen for their help with the TEM and SEM sample processing, respectively, and Martha G. Aguilar-Romero for her secretarial assistance. We would also thank Alicia Chagolla for her support with the LC-MS/MS identification in the Proteomics facility at CINVESTAV-Irapuato, Mexico and Daniel Ortega-Arroyo for manuscript editing.

Financial support. This work was partially supported by CINVESTAV-IPN and by the Consejo Nacional de Ciencia y Tecnología (CONACYT) Mexico (RA, grant numbers 162123 and 153093), CONACYT Mexico LARR received a Ph.D. scholarship number 338864 from CONACYT, MSHG received a Ph.D. scholarship number 375264 from CONACYT and SRC received a Ph.D. scholarship number 780847 from CONACYT.

Conflict of interest. None.

Ethical standards. Not applicable.

References

Abcam Protocols (2018) https://docs.abcam.com/pdf/protocols/apoptosis-dna-fragmentation-analysis-protocol.pdf

Alvarez-Sánchez ME, Avila-González L, Becerril-García C, Fattel-Facenda LV, Ortega-López J and Arroyo R (2000) A novel cysteine proteinase (CP65) of *Trichomonas vaginalis* involved in cytotoxicity. *Microbial Pathogenesis* **28**, 193–202.

Alvarez-Sánchez ME, Solano-González E, Yañez-Gómez C and Arroyo R (2007) Negative iron regulation of the CP65 cysteine proteinase cytotoxicity in *Trichomonas vaginalis*. *Microbes and Infection* **9**, 1597–1605.

Arroyo R and Alderete JF (1989) *Trichomonas vaginalis* surface proteinase activity is necessary for parasite adherence to epithelial cells. *Infection and Immunity* **57**, 2991–2997.

Arroyo R, Cárdenas-Guerra RE, Figueroa-Angulo EE, Puente-Rivera J, Zamudio-Prieto O and Ortega-López J (2015) *Trichomonas vaginalis* cysteine proteinases: iron response in gene expression and proteolytic activity. *Biomedical Research International* **2015**, 946787.

Cárdenas-Guerra RE, Arroyo R, Rosa de Andrade I, Benchimol M and Ortega-López J (2013) The iron-induced cysteine proteinase TvCP4 plays a key role in *Trichomonas vaginalis* haemolysis. *Microbes and Infection* **15**, 958–968.

Charras GT (2007) A short history of blebbing. *Journal of Microscopy* **23**, 466–478.

Elmore S (2007) Apoptosis: a review of programmed cell death. *Toxicologic Pathology* **35**, 495–516.

Figueroa-Angulo EE, Rendón-Gandarilla FJ, Puente-Rivera J, Calla-Choque JS, Cárdenas-Guerra RE, Ortega-López J, Quintas-Granados LI, Alvarez-Sánchez ME and Arroyo R (2012) The effects of environmental factors on the virulence of *Trichomonas vaginalis*. *Microbes and Infection* **14**, 1411–1427.

Figueroa-Angulo EE, Calla-Choque JS, Mancilla-Olea MI and Arroyo R (2015) RNA-binding proteins in *Trichomonas vaginalis*: atypical multifunctional proteins involved in a posttranscriptional iron regulatory mechanism. In: "RNA-binding proteins – structure, function, networks and disease". *Biomolecules* **5**, 3354–3395.

Fiori PL, Rappelli P, Rocchigiani AM and Cappuccinelli P (1993) *Trichomonas vaginalis* haemolysis: evidence of functional pores formation on red cell membranes. *FEMS Microbiology Letters* **109**, 13–18.

Hernández HM, Marcet R and Sarracent J (2014) Biological roles of cysteine proteinases in the pathogenesis of *Trichomonas vaginalis*. *Parasite* **21**, 54.

Hernandez-Gutierrez R, Ortega-López J and Arroyo R (2003) A 39-kDa cysteine proteinase CP39 from *Trichomonas vaginalis*, which is negatively affected by iron may be involved in trichomonal cytotoxicity. *Journal of Eukaryotic Microbiology* **50**, 696–698.

Hernández-Gutiérrez R, Avila-González L, Ortega-López J, Cruz-Talonia F, Gómez-Gutierrez G and Arroyo R (2004) *Trichomonas vaginalis*: characterization of a 39-kDa cysteine proteinase found in patient vaginal secretions. *Experimental Parasitology* **107**, 125–135.

Huang KY, Chen YY, Fang YK, Cheng WH, Cheng CC, Chen YC, Wu TE, Ku FM, Chen SC, Lin R and Tang P (2014) Adaptive responses to glucose restriction enhance cell survival, antioxidant capability, and autophagy of the protozoan parasite *Trichomonas vaginalis*. *Biochimie and Biophysical Acta* **1840**, 53–64.

Huang KY, Ong SC, Wu CC, Hsu CW, Lin HC, Fang YK, Cheng WH, Huang PJ, Chiu CH and Tang P (2017) Metabolic reprogramming of hydrogenosomal amino acids in *Trichomonas vaginalis* under glucose restriction. *Journal of Microbiology and Immunology Infections*. pii: S1684-1182(17)30241-4. doi: DOI.ORG/10.1016/J.JMII.2017.10.005.

Kummer S, Hayes GR, Gilbert RO, Beach DH, Lucas JJ and Singh BN (2008) Induction of human host cell apoptosis by *Trichomonas vaginalis* cysteine proteases is modulated by parasite exposure to iron. *Microbial Pathogenesis* **44**, 197–203.

Lubick KJ and Burgess DE (2004) Purification and analysis of a phospholipase A2-like lytic factor of *Trichomonas vaginalis*. *Infection and Immunity* **72**, 1284–1290.

Mancilla-Olea MI, Ortega-López J, Figueroa-Angulo EE, Avila-González L, Cárdenas-Guerra RE, Miranda-Ozuna JFT, González-Robles A, Hernández-García MS, Sánchez-Ayala L and Arroyo R (2018) *Trichomonas vaginalis* cathepsin D-like aspartic proteinase (Tv-CatD) is positively regulated by glucose and degrades human hemoglobin. *International Journal of Biochemistry and Cell Biology* **97**, 1–15.

Midlej V and Benchimol M (2010) *Trichomonas vaginalis* kills and eats–evidence for phagocytic activity as a cytopathic effect. *Parasitology* **137**, 65–76.

Mills JC, Stone NL and Pittman RN (1999) Extranuclear apoptosis. *The role of the cytoplasm in the execution phase. Journal of Cell Biology* **146**, 703–708.

Miranda-Ozuna JFT, Hernández-García MS, Brieba LG, Benítez-Cardoza CG, Ortega-López J, González-Robles A and Arroyo R (2016) The glycolytic enzyme triosephosphate isomerase of *Trichomonas vaginalis* is a surface-associated protein induced by glucose that functions as a laminin- and fibronectin-binding protein. *Infection and Immunity* **84**, 2878–2894.

Petrin D, Delgaty K, Bhatt R and Garber G (1998) Clinical and microbiological aspects of *Trichomonas vaginalis*. *Clinical Microbiology Reviews* **11**, 300–317.

Poole DN and McClelland RS (2013) Global epidemiology of *Trichomonas vaginalis*. *Sexually Transmitted Infections* **89**, 418–422.

Puente-Rivera J, Ramón-Luing LA, Figueroa-Angulo EE, Ortega-López J and Arroyo R (2014) Trichocystatin-2 (TC-2): an endogenous inhibitor of cysteine proteinases in *Trichomonas vaginalis* is associated with TvCP39. *International Journal of Biochemistry and Cell Biology* **54**, 255–265.

Quan JH, Kang BH, Yang JB, Rhee YE, Noh HT, Choi IW, Cha GH, Yuk JM and Lee YH (2017) *Trichomonas vaginalis* induces SiHa cell apoptosis by NF-kB inactivation *via* reactive oxygen species. *Biomed Research International* **2017**, 3904870.

Ramón-Luing LD, Rendón-Gandarilla FJ, Puente-Rivera J, Ávila-González L and Arroyo R (2011) Identification and characterization of the immunogenic cytotoxic TvCP39 proteinase gene of *Trichomonas vaginalis*. *International Journal of Biochemistry and Cell Biology* **43**, 1500–1511.

Rendón-Gandarilla FJ, Ramón-Luing LA, Ortega-López J, Rosa de Andrade I, Benchimol M and Arroyo R (2013) The TvLEGU-1, a legumain-like cysteine proteinase, plays a key role in *Trichomonas vaginalis* cytoadherence. *Biomedical Research International* **2013**, 561979.

Sánchez-Rodríguez DB, Ortega-López J, Cárdenas-Guerra RE, Reséndiz-Cardiel G, Chávez-Munguía B, Lagunes-Guillen A and Arroyo R (2018) Characterization of a novel endogenous cysteine proteinase inhibitor, trichocystatin-3 (TC-3), localized on the surface of *Trichomonas vaginalis*. *International Journal of Biochemistry and Cell Biology* **102**, 87–100.

Singh M, Sharma H and Singh N (2007) Hydrogen peroxide induces apoptosis in HeLa cells through mitochondrial pathway. *Mitochondrion* **7**, 367–373.

Solano-González E, Burrola-Barraza E, León-Sicairos CR, Avila-Gónzalez L, Gutiérrez-Escolano L, Ortega-López J and Arroyo R (2007) The trichomonad cysteine proteinase TVCP4 transcript contains an iron-responsive element. *FEBS LETTERS* **581**, 2919–2928.

Sommer U, Costello CE, Hayes GR, Beach DH, Gilbert RO, Lucas JJ and Singh BN (2005) Identification of *Trichomonas vaginalis* cysteine proteases that induce apoptosis in human vaginal epithelial cells. *Journal of Biological Chemistry* **208**, 23853–23860.

Stafkova J, Rada P, Meloni D, Zarsky V, Smutna T, Zimmann N, Haranta K, Pompach P, Hrdy L and Tachezy J (2018) Dynamic secretome of *Trichomonas vaginalis*: Case study of β-amylases. *Molecular Cellular Proteomics* **17**, 304–320.

Torres-Romero JC and Arroyo R (2009) Responsiveness of *Trichomonas vaginalis* to iron concentrations: Evidence for a post-transcriptional iron regulation by an IRE/IRP-like system. *Infection, Genetics and Evolution* **9**, 1065–1074.

Tovy A, Hertz R, Siman-Tov R, Syan S, Faust D, Guillen N and Ankri S (2011) Glucose starvation boosts *Entamoeba histolytica* virulence. *PLoS Neglected Tropical Diseases* **5**, e1247.

https://doi.org/10.1017/S0031182019000209 Published online by Cambridge University Press